Journal of Nuclear Materials 390–391 (2009) 478–481

Contents lists available at ScienceDirect

Journal of Nuclear Materials

journal homepage: www.elsevier.com/locate/jnucmat

Effect of disruptions on fuel release from JET walls

V. Philipps [a,*], M. Freisinger [a], A. Huber [a], T. Loarer [b], JET EFDA contributors [c]

[a] Institute of Energy Research, IEF-4: Plasma Physics, Forschungszentrum Jülich GmbH, EURATOM Association, Trilateral Euregio Cluster, D-52425 Jülich, Germany
[b] Association EURATOM-CEA, DSM-DRFC, CEA Cadarache, 13108 St Paul lez Durance, France
[c] JET-EFDA, Culham Science Centre, OX14 3DB Abingdon, UK

ARTICLE INFO

PACS:
52.40.Hf

ABSTRACT

The amount and temporal behaviour of the fuel release from the JET walls has been analysed for normal and disruptive shots during the JET SRP divertor campaign (2002–2004 with about 8000 plasma shots). The averaged fuel release in the first 700 s after the shots for nondisruptive shots is 1.8×10^{22} atoms compared with an averaged value of 3.7×10^{22} for the disruptive shots. A clear and approximately linear increase of the released particles with the plasma stored energy at the time of disruption is found. Non-disruptive and disruptive shots can be clearly separated from the temporal evolution of the fuel release showing a slow particle release after nondisruptive and an instantaneous release after disruptive shots indicating thermally induced particle desorption after disruptions.

1. Introduction

The magnitude and control of long term fuel retention are among the most critical issues for future fusion devices aiming to operate under steady state conditions [1]. This topic is intensively investigated at the Joint European Tokamak, JET, which currently operates with full carbon walls and regular Be evaporation conditioning. The fuel retention is both analysed by post mortem analysis of wall tiles [2] taken out after JET campaigns and by gas balance measurements under identical conditions for typically 10–20 shots [3]. From post mortem analysis it is found that the majority of the retained fuel is incorporated in redeposited carbon/Be layers formed mainly on the plasma facing sides and remote areas of the inner divertor, but also in dedicated areas in the outer divertor and layers growing on side areas of the main chamber protection limiters. The campaign averaged fuel retention evaluated from those data is about 2×10^{20} D/s (1). Gas balance measurements have been performed in JET in L mode, type III and Type I Elmy-H mode conditions in different plasma configurations, yielding consistent fuel retention rates between about 8 and 20×10^{20} D/s [4]. These data are obtained from the balance of injected and fuel regenerated just about one hour after plasma operation and does thus not include the long term release tail of the fuel release which is e.g. reported in this paper and also not other actions which can lead to additional fuel release like wall conditioning and in particular disruptions which appear in JET typically at a rate of about 10%. Disruptions are known to release additional fuel from the walls [5]. Controlled release of the fuel by disruptions has been also proposed as a possible method to control the fuel inventory in ITER by applying frequently controlled mitigated disruptions [6]. In order to address these questions, this paper analyses the amount and characteristic of the fuel release from disruptions in JET and compares it with normally terminated shots.

2. Experimental

The particle release from the walls has been analysed using the conventional penning gauges installed at the main wall near the port plugs for the main chamber pumping system. Both long term data up to 700 s after the shot and short term signals from the same penning gauge but with a higher sampling rate have been used. To evaluate quantitatively the amount of particle release, the effective pumping speed and the penning calibration must be known. For this, dry run gas injections have been analysed which are performed routinely in the morning before plasma operation with the torus pumping provided by the main chamber turbomolecular pump and the divertor cryogenic pumps. The pumping speed has been evaluated for each injection from the logarithmic decay of the pressure and compared with the temporal integral of the gas pressure and the amount of injected gas as given by the absolutely calibrated gas injection system in JET. This yields the penning gauge calibration according to

$$\int P dt = Q/s \tag{1}$$

with Q the total amount of injected particles (mbar), P the measured pressure (mbar) and s (l/s) the pumping speed evaluated from the decay of the pressure according to

* Corresponding author.
E-mail address: v.philipps@fz-juelich.de (V. Philipps).

0022-3115/$ - see front matter © 2009 Elsevier B.V. All rights reserved.
doi:10.1016/j.jnucmat.2009.01.049

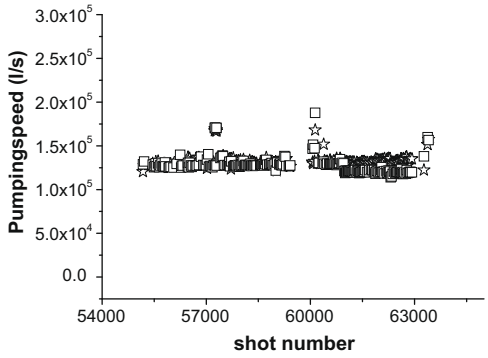

Fig. 1. Pumping speeds evaluated from pressure decay of gas injection (squares) and from integrated particle balance using the penning gauge calibration (stares) for the C5–C14 campaign. Pumping by turbopumps and divertor cryopump.

$$p(t) = Po * \exp(s/V * t) \quad (2)$$

with V the JET volume taken as 185 m^3. Fig. 1 compares the pumping speeds for all dry gas injections during the campaign evaluated from the pressure decay, which are independent on the penning calibration with those evaluated from Eq. (1) which depends on the actual penning calibration. As seen, the calibration given by the JET data acquisition system provides a reliable calibration over all the campaign. The mean pumping speed evaluated from the pressure decays is 127 m^3/s while the mean value derived from the gas balance results in 132 m^3/s, deviating only by 4%. The scatter of the data results from the fast pressure decay and the fact that often multiple gas injection pulses are performed on a short time scale which leads sometimes to a small cumulative increase of the background pressure. It is important to note that the present penning calibration accounts for the pressure of equivalent atoms although hydrogen molecules constitutes the pressure in those dry runs and also predominantly after plasma discharges.

With beam heated plasmas, the NB injector cryogenic pumps pump in addition with a pumping speeds of about 40 m^3/s for each of both NBI injector systems in JET, as evaluated in several earlier investigations [7]. To ensure exact knowledge of the actual pumping speed, this analysis restricted to shots where both NBI systems were operating and for which pressure data up to 700 s after the plasma were available. This restricted the database to about 1100 shots out of about 7300 shots in this JET campaign (C5–C14) which survived the plasma ramp up (nonsustained breakdowns have been omitted). Table 1 gives the fuel injection and number of disruptions over the whole campaign and in the present database. As can be seen the database represents the campaign averaged conditions quite well.

3. Results

3.1. Fuel release from nondisruptive shots

As shown earlier [8] the pressure evolution after nondisruptive shots is determined by the temporal evolution of the fuel release from the walls with minor influence of the vacuum time constants under the strong JET pumping conditions. During the plasma operation, the neutral pressure measured at the walls remains low up

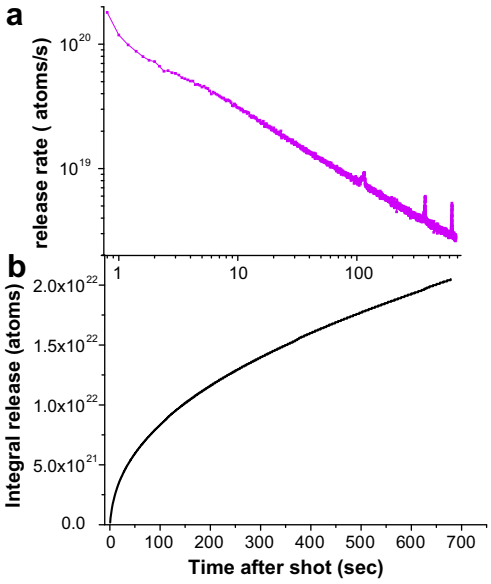

Fig. 2. (a) Temporal decay of the particle release of a nondisruptive shot in a log–log plot. (b) Integral particle release.

to the very end of the plasma current ramp down and then increases sharply. The initial release rate just after the end of a shot in JET is several 10^{21} D/s and must represent the total recycled particle flux just during the last time of the shot. The release then drops fast with a temporal characteristic as described below. The release results from the property of graphitic wall surfaces to store hydrogen temporarily by building up a 'dynamic inventory' in the carbon plasma facing components. This dynamic wall pumping enables also the soft landing of the plasma since active pumping during plasma ramp down is low (limiter plasma configuration) and, if absent, lead to a density limit disruption at the plasma current ramp down as normally observed for He plasma operation. The temporal evolution of the released flux $Q(t)$ after the plasma end is given by

$$Q(t) = dp/dt * V + p * s \quad (3)$$

with the usual quotations as used in Eqs. (1) and (2). Fig. 2a shows the release flux in a log–log plot and Fig. 2b the cumulative integrated particle release for a typical nondisruptive discharge at JET. The release follows a uniform power law similar as already discussed in [8], but with a slightly lower power law exponent. The integrated particle release for all nondisruptive shots has been evaluated up to 5, 10, 50 and 500 s after the discharge. Fig. 3 shows the mean values of the fraction of the integral release normalised to the release up to 500 s for all nondisruptive shots. The integral particle release follows a power law $\approx t^{-0.41}$, corresponding to a particle release rate $Q(t) \sim t^{0.59}$. This is somewhat slower as discussed in (8) but it should be noted that, in the present analysis, the pressure rise from the cumulative particle release from previous shots has not been subtracted but has been in (8). This cumulative release slows down the decay of the fuel release for a particular discharge as discussed in more detail in (8). The data show that the fuel is released continuously after the end of data reading (700 s). Fig. 4 shows the

Table 1
Total database of the JET campaign (JET SRP) and the reduced database used in the present analysis.

	Number of shots	Number of disruptions	Av. injection/shot (atoms)	Integrated injection (atoms)
Overall campaign	7297	709 (9.7%)	7.12×10^{22}	5.2×10^{26}
Present database	1091	112 (10%)	9.7×10^{22}	1.05×10^{26}

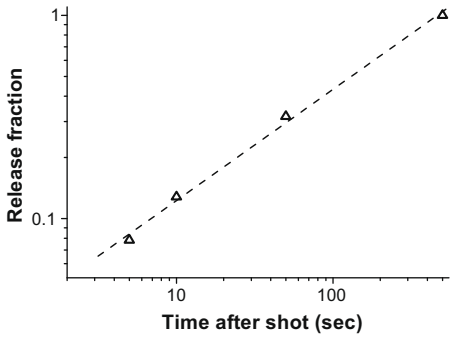

Fig. 3. Fraction of release (normalised to the release up to 500 s) at different times after the shot for all nondisruptive shots. The release follows $R(t) \sim t^{0.41}$.

absolute release for all shots until 700 s resulting in a mean value of 1.8×10^{22} /shot. Assuming the temporal behaviour to continue and a mean time delay between shots of 1800 s, the total release in between shots increase by about 40% from 1.8 to 2.5×10^{22} D-atoms/shot. This amount corresponds to a dynamic inventory of about 10^{20} D/cm^2 if distributed uniformly over the JET first wall area ($\approx$200 m^2). This must be compared with the saturation value of fuel retained in the plasma interaction zone of carbon erosion areas which is about 10^{21} D/cm^2 [9]. Thus the dynamic inventory in graphitic surfaces is about 10% of the saturation value, noticeable at the JET base wall temperature of around 200 °C.

It should be noted that the particle release must decay faster after some time since the integral of the power law release dependence is infinite while the fuel reservoir in the walls certainly is finite. However, the transition to a faster decay could not be identified clearly so far.

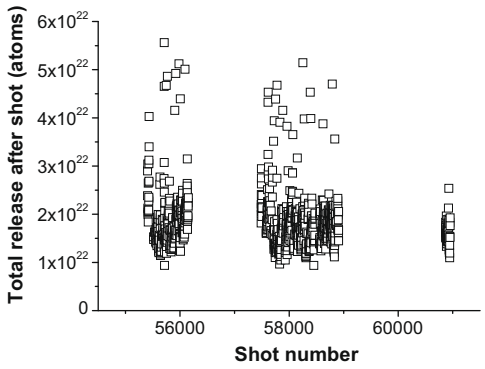

Fig. 4. Particle release integrated up to 700 s after the shot for all nondisruptive shots.

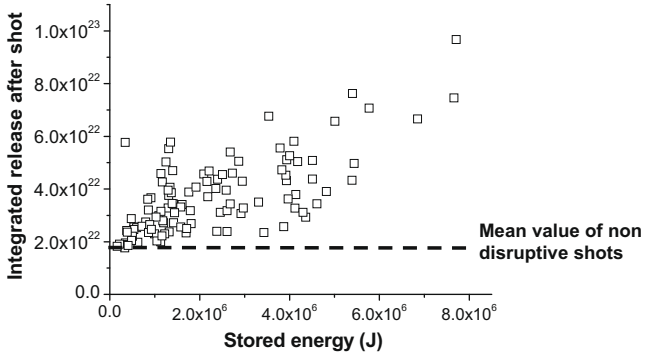

Fig. 5. Particle release integrated up to 700 s after the shot for all disruptive shots.

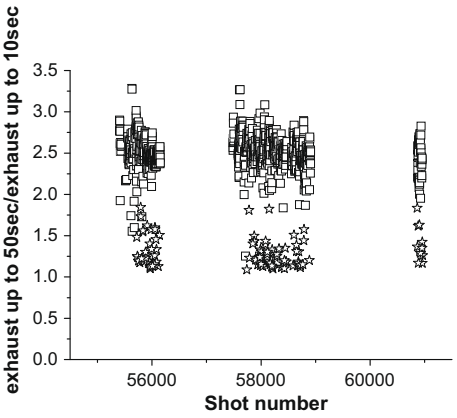

Fig. 6. Ratio of particle release after the shot integrated up to 50 s to that up to 10 s for nondisruptive (squares) and disruptive shots (stares).

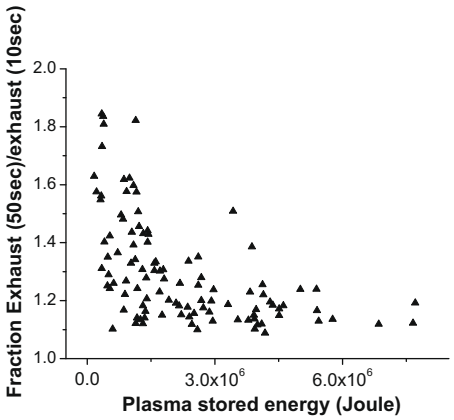

Fig. 7. Ratio of particle release after the shot integrated up to 50 s to that up to 10 s for all disruptive shots versus stored energy before the disruption.

3.2. Fuel release after disruptive shots

Fig. 5 shows the total amount of fuel released up to 700 s for all disruptions in the database versus the stored energy just before the disruption. The release increases continuously with increasing plasma energy at the disruption with a mean particle release of 3.7×10^{22} atoms/shot, twice of that for normal shots, and a maximum release up to 10^{23}/shot. Fig. 6 shows the fraction of fuel released up 50 s to that released in the first 10 s for all normal shots and for all disruptions. It can be seen that the temporal release characteristic for all nondisruptive shots is quite similar, with a slow decrease of the release with time. The disruption data show that most of the fuel is released in the first 5 s after the disruption, in contrast to the normal shots. Fig. 7 shows this fraction again for the disruptive shots plotted against the stored energy demonstrating that the fraction of fast released particles increases with stored energy.

4. Summary and discussion

The fuel release after nondisruptive JET shots under the present carbon wall conditions (and at a wall base temperature of 200 °C) is determined by the dynamic trapping of fuel in the plasma loaded graphitic surfaces. The total amount of the dynamic inventory is several about 3×10^{22} corresponding to about 2×10^{20} D/m^2 if uniformly distributed over the JET wall area. The dynamic inventory depends also only weakly on the total amount of fuelling/shot

indicating that this dynamic inventory is close to saturation in JET and could not be increased much if JET would e.g. operate with longer plasma pulses (higher wall particle fluencies). The dynamically retained fuel is then slowly released with a quite uniform power law $\sim t^n$ law with an exponent $n = -0.6$. This dynamic inventory is also responsible for the dynamic wall pumping and enables e.g. the plasma soft landing in the limiter ramp down phase of JET.

In disruptive shots additional fuel is released which increases linearly with the stored energy at the time of disruption. The averaged fuel release is only about twice that for normal shots but maximum values at the highest stored energies up to 5 times the normal release are observed. The temporal behaviour of the disruptive fuel release follows largely the time decay of the vacuum pump down time showing that the fuel is released instantaneously at the disruption. The most likely process for this is thermal desorption from overheated wall areas due to the disruptive power loss to the walls. For the possible use of controlled disruptions as a possible method for *T* removal, only the disruptive heating of carbon deposits is effective since the release from erosion-dominated areas will be refilled in subsequent shots while thermal release from deeper regions in deposits will occur which will not be refilled. The total amount of fuel in erosion areas in JET is estimate to several 10^{23} fuel atoms (saturation at $10^{21}/m^2 \times 200\,m^2$ wall area) which is reached in the largest disruptions investigated here. This indicates that fuel release from codeposits contributes largely since a disruptive heating of large areas of the first wall is not possible in JET. A possible release is from deposits at the side areas of the main chamber protection limiters. If we attribute the average additional release of $\approx 2 \times 10^{22}$ atoms/disruption as observed here only to the thermal release from codeposits, assuming a disruption frequency of 10%, a total additional fuel release of 30 g can be estimated per typical JET campaign. This is in the range of the campaign averaged retention observed by post mortem analysis, e.g. 60 g in the SRP divertor campaign [10]. The fraction of fuel retention observed on the plasma wetted deposits in JET is typically 0.1–0.2 D/C+Be but with higher values on plasma hidden areas (0.5–1 D/C, (9)) indicating that fuel release occurs by disruption heating of the deposits on plasma wetted surfaces, in particular on areas away from the divertor strike zones, where also ELM induced release plays a role. Thus larger and controlled disruptions can contribute to reduce the fuel reservoir in deposits on plasma wetted surfaces, but also redistribute material from plasma wetted to shadowed areas where cleaning is more difficult. This redistribution in disruptions was recently observed in JET with QMB deposition detectors [11].

Acknowledgements

This work, supported by the European Communities under the contract of Association between EURATOM and FZJ, was carried out within the framework of the European Fusion Development Agreement. The views and opinions expressed herein do not necessarily reflect those of the European Commission.

References

[1] ITER Physics Basis, Nucl. Fus. 47 (2007).
[2] J.P. Coad et al., Nucl. Fus. 46 (2) (2006) 350.
[3] T. Loarer, C. Brosset, J. Bucalossi, Nucl. Fus. 47 (2007) 1112.
[4] T. Loarer, N. Bekris, S. Brezinsek et al., Fuel Retention in Tokamaks, these Proceedings.
[5] B. Lipschultz, D.G. Whyte, J. Irby et al., Hydrogenic Retention in a High-Z Plasma Facing Component: Alcator C-Mod, these Proceedings .
[6] G. Counsell, P. Coad, C. Grisola, et al., Plasma Phys. Control. Fus. 48 (2006) B189.
[7] J. Bucalossi et al., Particle Balance Studies in JET 28th Eur. Conf. on Controlled Fusion and Plasma Physics (Funchal, 18–22 June 2001), vol. 25A (ECA), 2001, p. 1629.
[8] V. Philipps, J. Ehrenberg, J. Vac. Sci. Technol. A 11 (2) (1993).
[9] See e.g. P. Wienhold, V. Philipps, et al., J. Nucl. Mater. 313–316 (2003) 311.
[10] J. Likonen, J.P. Coad, D.E. Hole, et al., J. Nucl. Mater. 390–391 (2009) 631.
[11] A. Kreter, S. Brezinsek, J.P.Coad et al, Dynamics of Erosion and Deposition in Tokamaks, these Proceedings.